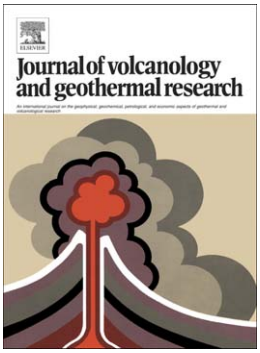

Tephra layers along the southern Tyrrhenian coast of Italy: Links to X-5 & X-6 using volcanic glass geochemistry

P. Donato, P.G. Albert, M. Crocitti, R. De rosa, M. Menzies

PII: S0377-0273(16)30003-8
DOI: doi: 10.1016/j.jvolgeores.2016.02.023
Reference: VOLGEO 5773

To appear in: *Journal of Volcanology and Geothermal Research*

Received date: 18 November 2015
Revised date: 11 February 2016
Accepted date: 24 February 2016

Please cite this article as: Donato, P., Albert, P.G., Crocitti, M., De rosa, R., Menzies, M., Tephra layers along the southern Tyrrhenian coast of Italy: Links to X-5 & X-6 using volcanic glass geochemistry, *Journal of Volcanology and Geothermal Research* (2016), doi: 10.1016/j.jvolgeores.2016.02.023

Tephra layers along the southern Tyrrhenian coast of Italy: links to X-5 & X-6 using volcanic glass geochemistry

P. DONATO[1]*, P.G. ALBERT[2,4], M. CROCITTI[3], R. DE ROSA[1], M. MENZIES[4]

1DiBEST Università della Calabria, Via P. Bucci 15/B, 87036 Rende (CS), Italy paola.donato@unical.it

2RLAHA, University of Oxford, UK.

3 Università di Bari, Via Orabona 4, 70125 Bari (BA), Italy

4Earth Sciences, RHUL, UK

Abstract: We present the geochemistry of glass fragments from three visible tephra layers outcropping in Southern Italy. Two tephra deposits (LeS1 and LeS2), outcropping in the Palinuro area (Cilento, Southern Italy), correspond stratigraphically to the CIL1 and CIL2 tephra units (Giaccio et al., 2012), respectively; in turn these are correlated with the X-5 (ca. 105 ka) and X-6 (ca. 108 ka) marine tephra markers on the basis of their major element glass compositions. In order to reinforce these tephra correlations we examine both their major and trace element glass compositions. LeS1 compositions were compared with other correlatives of the X-5 tephra layer (POP3 [Sulmona basin], TM-25 [Lago Grande di Monticchio (LGdM)], CIL1 [Palinuro]) from the central Mediterranean. Our data validate a correlation of the Palinuro tephra layer, LeS1, to the X-5 correlatives. The Palinuro tephra deposit, LeS2, has glass compositions which correspond precisely with correlatives of the X-6 marker tephra (CIL2 [Palinuro], TM-27 [LGdM], I-9 [Ionian Sea] and PRAD 2812 [PRAD1-2, Adriatic Sea]). A tephra in the Valle del Crati (Calabria) appears to overlap in composition with the LeS2 tephra, indicating a probable correlation with the X-6 marker. These new data provide a detailed geochemical characterisation of two widespread marker horizons and are crucial for establishing precise correlations of sedimentary archives across the central Mediterranean region.

Keywords: Glass analyses, LA-ICP-MS, MIS 5 tephra markers, tephrostratigraphy

1. Introduction

Explosive volcanic eruptions are responsible for the widespread dispersal of ash (particle diameter <2 mm) or tephra, and its near instantaneous deposition provides important stratigraphic markers recorded in a range of sedimentary records. Over the past few decades tephrostratigraphic investigations of marine and terrestrial sedimentary archives have played a fundamental role in stratigraphically constraining and synchronising Quaternary successions in the Mediterranean region. The central Mediterranean is particularly well placed to utilise tephra markers owing to an abundance of volcanoes, with differing geochemical signatures, that have been repeatedly active during the last 200 ka (e.g. Keller et al., 1978; Paterne et al., 1986,1988,2008; Sulpizio et al., 2003; Giaccio et al., 2008 a and b, 2009,2012;Wulf et al., 2004,2012; Siani et al., 2004; Lowe et al., 2007; Zanchetta et al., 2008). Key tephrostratigraphic markers rely upon (1) a widespread dispersal from a volcanic source and; 2) their chemical and petrographic fingerprints being well characterised, enabling the identification of diagnostic features unique to individual eruptions. Where a tephra can be attributed to a specific eruption of known age it can provide an important chronological marker. Linking distal tephra deposits to dated (i.e., $^{40}Ar/^{39}Ar$; ^{14}C) proximal tephra units is not always possible, with resurgent explosive activities often destroying the volcanic stratigraphy of older eruptive events (Di Vito et al., 2008; Zanchetta et al., 2008; Albert et al., 2015). In these instances the dating of an eruption must be determined in the distal realm through direct dating (e.g.,$^{40}Ar/^{39}Ar$; Smith et al., 2011a; Giaccio et al., 2012) or indirect dating (e.g., varve chronologies; Wulf et al., 2004,2008,2012). Through rigorous geochemical correlations the age of distal tephra markers can then be exported between sedimentary archives.

Both proximal-distal and distal-distal tephra correlations are increasingly underpinned by volcanic glass geochemistry. Furthermore it is widely accepted that distal tephra layers should be correlated to proximal glass chemistries rather than whole rock compositions because proximal tephra deposits are often richer in phenocryst phases. In contrast during wind transport, density sorting means that the distal ash deposits are enriched in the light, glassy components, and depleted in the heavier, crystalline or lithic fractions. As a consequence the composition of a distal tephra is not directly comparable to proximal, crystal rich, whole rock compositional data as this can lead to erroneous correlations (see Tomlinson et al., 2012 a and b). It is also recognised that major element compositions of volcanic glass cannot always be sufficient for precise correlations, this is because the products of the same magmatic source can produce indistinguishable major element compositions through successive eruptions (Allan et al., 2008; Giaccio et al., 2008a; Tomlinson et al., 2012a). Moreover, as the tephra layers can often show a certain degree of alteration, their content in mobile elements, e.g. alkalis, can be modified by the weathering process. More recently some authors have proposed that tephra correlations can be strengthened by assessing the trace element concentrations in the glass shards and minerals (De Rosa et al., 2008; Smith et al., 2011a and b; Tomlinson et al., 2012 a and b; Albert et al., 2012). The advantage in using trace elements is that their concentrations are generally more variable between eruptions from the same volcanic source owing to their greater sensitivity to fractionation processes (i.e., Allan et al., 2008; Albert et al., 2015); in addition, some trace element concentrations (i.e. immobile High Field Strength Elements) are less susceptible to modification by weathering processes.

The X-5 and X-6 tephra represent two key Late Quaternary central Mediterranean tephrostratigraphic markers within the post Interglacial MIS 5e period (MIS 5a-d or Early Weichselian) owing to their widespread distribution across the region (Fig. 1). These tephra layers were first identified within Ionian Sea marine cores (Keller et al., 1978),

below sapropel 4, their trachytic compositions linking them to Campanian volcanic activity. The Ionian Sea X-6 and X-5 tephras have been successively recognised in many Mediterranean marine, lacustrine and terrestrial sequences. Paterne et al. (2008) recognised the two levels in the Tyrrhenian and Ionian Sea cores; the C-27 is correlated with X-5, whilst C-31 corresponds to X-6. X-5 and X-6 are also thought to occur interbedded within the proximal pyroclastics of Salina and Panarea (Aeolian Islands, Lucchi et al., 2013). The X-6 has also been reported in central Adriatic Sea (Bourne et al.,2015), in the Ionian Sea (Insinga et al., 2014) and in the Balkan region (Sulpizio et al., 2010).

The X-6 and X-5 tephra are also recorded in the annually laminated lacustrine sequence of Lago Grande di Monticchio (LGdM; Monte Vulture, Southern Italy). TM-27 is the recognised correlative of X-6 tephra at LGdM (Wulf et al., 2012), and following a recent re-appraisal TM-25 is considered the LGdM equivalent of the X-5 tephra (Wulf et al., 2012). The X-5 had been previously assigned to the slightly younger LGdM tephra layers TM-24a and b. The varve chronology of LGdM means that these eruptions can be independently dated (Table 1). In a recent paper the two tephra markers have been found in the subaerial environments of southern and central Italy, both the Sulmona basin and along the Cilento Coast (Giaccio et al., 2012; Regattieri et al., 2015). Direct and indirect age determinations presented for the proposed distal equivalents of these two tephra markers are consistent with their stratigraphic positions within sediments deposited immediately following the termination of the Last Interglacial (MIS 5e) (Table 1).

The composition of X-5 tephra is trachytic (Wulf et al. 2012; Giaccio et al., 2012), while the X-6 has been reported as a trachy-phonolite (e.g. Wulf et al., 2012; Iorio et al., 2014) to trachyte (Giaccio et al., 2012; Regattieri et al., 2015). Tephra correlations associated with the X-5 and X-6 tephra are predominantly underpinned by stratigraphy and major element glass chemistry (EDX or EMP), indeed only limited trace element data is currently

available for X-5 and X-6 correlatives. Such trace element data is crucial in helping to prevent erroneous tephra correlations, particularly if we consider the significant major element chemical overlap observed between the X-5 tephra and temporally similar tephra deposits. This is best demonstrated by the TM-24 and TM-25 layers recorded in the LGdM record.

In this paper we present major, minor and trace element chemistry for volcanic glasses from layers outcropping in two different areas of Southern Italy (Fig. 1). Two layers were sampled along the Cilento coast (Palinuro) and stratigraphically correspond to the two layers correlated with X-5 and X-6 tephra markers by Giaccio et al. (2012). The other sampled volcaniclastic deposit outcrops in the Valle del Crati, near the village of Tarsia (Northern Calabria, Cosenza province). This deposit was the subject of a previous investigation by Carobene et al. 2006, they attributed it to an eruption younger than42 ka.

The objectives of this study are to:

- Compare the volcaniclastic layers outcropping in the two different localities on the basis of the geochemistry of the glass fraction, in order to establish if a correlation between the two sequences is possible;
- Compare the results with the published correlatives of X-5 and X-6 Mediterranean tephra markers, in order to verify or refute existing correlations already suggested for the Palinuro levels;
- Provide new diagnostic trace element data for the Palinuro and Tarsia tephra deposits which are essential for strengthening future tephrostratigraphical studies in the Mediterranean region in the absence of well characterised proximal equivalents.

2. Cilento and Valle del Crati tephra layers

2.1 Cilento tephra layers

A tephra layer in the Cilento area was first identified by Mirigliano (1949) at Cala Bianca and Porto degli Infreschi. A Plio-Pleistocenic age was given to these deposits by Scandone and Lirer (1966). Near the town of Palinuro a lithic rich industry of Levalloisian-Mousterian type has been discovered at the base and top of the pyroclastic layer, thus allowing an attribution at epi-Wurm II to the deposit (Blanc and Segre, 1953; Lirer et al., 1967). The pyroclastic layer has its best exposure along the coast, near the village of Palinuro, where it is interbedded with the deposits of the post- Tyrrhenian regressive dune formation. Northward, near “Le Saline” the tephra layer is about 1 meter thick and is included in red loose sands and gravels (Lirer et al., 1967). Scandone and Lirer (1966) and Lirer et al. (1967) identified the source of these deposits in a submarine volcano placed in southern Tyrrhenian Sea, excluding a provenance from Vulture or Campanian volcanoes.

In the same area Marciano et al. (2008) identified several tephra layers with an age between 200 ka and 70 ka. In particular, a layer correlated with the Campanian X-6 tephra has been recognised in two outcrops: one close to Palinuro, 0.5 to 1 meter thick (corresponding to the level described by Scandone and Lirer, 1967), and another northward, near San Marco di Castellabate.

Finally, at the locality “Le Saline” Giaccio et al. (2012) recognized a further volcaniclastic layer (CIL1), about one meter thick, above and separated by an incipient palaeosol from the lower CIL2 (the X-6 as described by Marciano et al., 2008). In their work the authors correlate this level with the X-5 tephra on the basis of its stratigraphic position and the major element geochemistry of the glasses.

The Cilento tephra layer correlated with X-6 marker (hereafter CIL2) is reddish-brown and made up of glass shards and aggregates and has a high content of crystals including feldspar, clinopyroxene, biotite, opaques and amphiboles. Glass compositions are trachytic, with a Na_2O/K_2O ratio of 0.6-0.8 (Marciano et al., 2008; Giaccio et al., 2012).

The uppermost layer (hereafter CIL1) is composed of white, very elongated and vesicular tubed pumices, which are trachytic in composition, and contain loose sanidine and biotite crystals (Giaccio et al., 2012).

Tephra layers correlated with those outcropping along the Cilento coast have also been observed along the Tyrrhenian coast of Basilicata and northern Calabria (Carobene et al., 1991; Critelli et al., 1995; Amelio et al., 1997; Scarciglia et al. 2006; Donato et al., 2013).

In this study the volcaniclastic layers were sampled in Le Saline locality, near Palinuro village (Fig. 2). A first deposit, named Le Saline 2 (LeS2), is a 1 m thick volcaniclastic layer interbedded in a deposit of reddish sands lying above the cross-bedded stratified sands. It has medium to coarse sand granulometry and a weathered top. On the basis of stratigraphic reconstructions this layer correlates with the CIL2 sample of Giaccio et al. (2012). A few tens of meters away from the sampled LeS2 unit, and stratigraphically above it is a second deposit, named LeSaline 1 (LeS1). It is massive and composed of white ash and can be stratigraphically correlated to CIL1 unit of Giaccio et al. (2012).

2.2. Valle del Crati tephra layer

A volcaniclastic deposit outcrops just outside the village of Tarsia (Calabria), in the western sector of the valley of the Crati river. The best outcrop is a few hundreds of meters from the cemetery of Tarsia. Carobene et al. (2006) studied the deposit in detail and dated it by thermal and optical stimulated luminescence, obtaining an age comprised between 42 and 25 ka. On the basis of the trachytic composition of the tephra, the authors proposed that the deposit is related to the volcanic activity of Ischia or Campi Flegrei.

The volcaniclastic layer is constrained between two colluvial levels, made up of a muddy matrix with angular clasts of metamorphic rocks, interpreted as a colluviums formed by the accumulation of debris flows at the base of the slope. The volcaniclastic deposit comprises of an ash massive and has a thickness ranging between 60 and 120 cm, a sandy grainsize

and a yellowish-white color (Fig. 2). The top of the deposit is rather cemented, probably because of pedogenesis; the intermediate and lower part is poorly cemented and contains few, scattered clasts of highly weathered, centimeter sized pumices. The deposit has been interpreted as the result of the re-mobilization of an original ash-fall level along the slope just after its deposition. For a complete description of the succession see Carobene et al. (2006).Two samples were picked, at the base and at the top of the deposit, named Lower Tarsia (LTa) and Upper Tarsia(UTa), respectively.

3. Analytical methods

3.1 Petrographic analysis and microanalysis of minerals

A petrographic study on bulk rock thin section has been conducted on the samples of the two localities. The compositions of main mineral phases in terms of major elements was determined by SEM-EDX. The used electron microscope is a FEG (Field Emission Gun) Quanta 200 F (FEI/Philips) equipped with an EDS system for X-ray microanalyses (EDAX GENESIS 4000 with Si/Li detector). Analysis was performed using a focused beam and an accelerating voltage of 20 kV. Quantitative analyses were obtained through the ZAF internal correction system. SEM-EDX analysis was carried out in the laboratories of the Department of Biology, Ecology and Earth Science of the University of Calabria, Italy.

3.2 Determination of glass composition

3.2.1 Electron Micro-Probe Analysis (EMPA)

Major element concentrations of individual glass shards of distal tephra samples were determined using JEOL JXA-8600 electron microprobe, equipped with 4 spectrometers and SamX software, at the Research Laboratory for Archaeology and the History of Art, University of Oxford. An accelerating voltage of 15 kV, low beam current (6 nA), and

defocused (10 µm) beam were used to minimize Na migration. Count times were 30 s on each peak, except for Na (10 s). The instrument was calibrated for each set of beam conditions using a suite of appropriate mineral standards. The calibration was verified using a range of secondary glass standards from the Max Planck Institute. Count rates were corrected using the PAP absorption correction method. Sample totals are normalised to 100 wt% in all plots and tables. Analytical precision is <10% relative standard deviation (%RSD) for analyses with concentrations >0.8 wt%. Error bars on plots represent the 2x standard deviation of replicate analyses of MPI-DING StHs6/80-G.

3.2.2 Laser Ablation Inductively Coupled Plasma Mass Spectrometry (LA-ICP-MS)

LA-ICP-MS analyses of glass shards of the distal tephra were performed using an Agilent 7500es coupled to a Resonetics 193 nm ArF excimer laser-ablation system (RESOlution M-50 prototype) with a two-volume ablation cell (Mueller et al., 2009) at the Department of Earth Sciences, Royal Holloway University of London. We used 34, 25 and 20 µm laser spots, depending on the size of the area available for analysis in different samples. The repetition rate was 5 Hz and the count time was 40 s (200 pulses) on the sample and 40 s on the gas blank (background). Concentrations were calibrated using NIST612 with ^{29}Si as the internal standard. Data reduction was performed manually using Microsoft Excel allowing removal of portions of the signal compromised by the occurrence of microcrysts. Full details of the analytical and data reduction methods are given in Tomlinson et al. (2010). Accuracies of ATHO-G and StHs6/80-G MPI-DING glass analyses are typically <5% for most elements and <10% for Nb, Pr, Eu, Gd, and Ta. Reproducibility of StHs6/80-G analyses is <5 RSD% for all trace elements. For consistency with EMPA error reporting, error bars on plots represent the 2 standards deviation of replicate analyses of StHs6/80-G. Relative standard errors (RSE) for LA-ICP-MS tephra samples analyses are typically <2 % for Rb, Sr, Zr, Nb, Ce, Pr; <5% for V, Y, Ba, La, Nd, Sm, Th, U, and <10% for Eu, Dy, Er, Yb, Lu.

4. Petrography and phase chemistry

The lowermost of Cilento tephra layers (LeS2) is mainly composed of highly vesiculated pumices, up to more than 1 mm in size, with rounded to stretched bubbles (Fig.3a). The crystalline component represents at least the 30 % of the deposit and it is mainly made up of coarse sanidine minerals (average composition $Ab_{44}An_4Or_{52}$). Plagioclase crystals are less abundant and smaller. Their average composition is $Ab_{58}An_{30}Or_{12}$ (supplementary data, Fig. 4a) Clinopyroxene is present both as colourless diopside and green, more Fe-rich crystals (Fig. 4b). Biotite and small leucite crystals are accessory phases.

The LeS1 tephra layer is finer and mainly composed of small pumices with highly stretched vesicles and glass shards (Fig. 3b). Coarser pumices with rounded to elongated bubbles are rare. Loose crystals are less abundant than in the LeS2 sample. Sanidine is the most abundant phase; its composition is very variable, with Or contents ranging from 90 to about 50 (Fig. 4a). Sanidine is followed, in order of abundance, by bytownite to andesine. Biotite, clinopyroxene and leucite are very rare.

The level outcropping near Tarsia is mainly composed of cuspidate and branched glass shards (Fig. 3c), representing the great majority of volcanic fraction. Rare coarser pumices also occur (Fig. 3d). Volcanic minerals are mainly dominated by sanidine, with average Or content of about 50, and subordinate andesinic plagioclase (Fig. 4a). Rare clinopyroxene (Fig. 4b), biotite and amphibole crystals are also present. Quartz grains and fragments of crystalline rocks form the non-volcanic fraction of the deposit.

5. Glass geochemistry

A TAS classification diagram reveals that the glasses of both volcaniclastic levels along the Cilento coastline are trachytes and phonolites, with LeS2 (lowermost level) glasses slightly more enriched in alkalis with respect to the LeS1 tephra (Fig. 5a). The chemical

differences between the two Cilento layers are more evident when the alkali ratios are assessed (Fig. 5b). LeS1 glasses have an average K_2O/Na_2O ratio of about 2.2, while the same ratio for LeS2 is always < 2 and many glasses show ratio values < 1. Thus the LeS1 glasses can be classified as being a high alkali ratio (HAR) tephra, whilst LeS2 is dominated by glass compositions showing a low alkali ratio (LAR). These two groupings can be distinguished on the basis of many major and trace elements. LeS1 glasses have higher contents of MgO, CaO and K_2O when compared to the LeS2 glasses, which, are more Na_2O-rich (Fig. 6). The LeS1 glasses are rather homogeneous, in contrast to the LeS2 glasses which show compositional bi-modality, particularly evident in the MgO and alkalis contents. Additionally, both the LILE and HFSE elements allow us to distinguish the tephra layers (Fig. 7) as the LeS2 glasses are depleted in Ba and Sr, yet enriched in Rb, Nb, Zr, Ta, Th, U and Light Rare Earth Elements (LREE, La and Ce, not shown).

Glass fragments from the Tarsia tephra deposit are trachytes to phonolites (Fig. 5a) and are very similar to those of the LeS2 layer, with a LAR ($K_2O/Na_2O<1$, Fig. 4b), MgO and CaO contents lower than 0.5 and 2 wt% respectively, relatively low K_2O (about 6.5 wt%) and high Na_2O (7 wt%) (Fig. 6). No significant variation in major elements is observed in the glasses from top to bottom. Trace element contents also point to a striking similarity between Valle del Crati and LeS2 layers, as they show the same, very low, concentration of Ba and Sr and elevated Rb, Nb, Zr and LREE (Fig. 7).

The normalized trace element diagram (Fig. 8a) confirms the compositional differences observed between LeS1 and LeS2/Tarsia levels, with the latter enriched in almost all the incompatible elements with the exception of Ba and Sr where significant depletions are observed. In the REE-chondrite normalized diagram (Fig. 8b) the two groups of glasses display almost parallel trends, with the LeS1 glass consistently showing lower contents in all the elements. An important difference is the almost complete absence of a Eu anomaly from the LeS1 glasses, a prominent feature of both the lower Le Saline tephra (LeS2) and

Tarsia glasses. For these samples the average value of Eu/Eu* (= $Eu_n/(Sm_nGd_n)^{0.5}$, where Eu_n, Sm_n and Gd_n are, respectively, the contents of Eu, Sm and Gd normalized to chondrites) is about 0.2 (Fig. 8b). Pronounced depletions in Ba, Sr and Eu in both the LeS2 and Tarsia glasses reflect significant levels of K-feldspar fractionation, a feature not observed in the LeS1 glasses. As already observed in the major elements compositions, the normalized trace elements and REE diagrams of the LeS2 glasses reveal a pronounced bimodality, with some glasses showing lower contents in most incompatible trace elements, together with higher K_2O and MgO contents. This bimodality reflects the occurrence, during the eruption, of two magma batches with different degrees of evolution dominated by the fractionation of mafic and potassic phases. Parallel REE profiles between LeS2-Tarsia and LeS1 might also be used to infer a genetic relationship between the two tephra deposits. All the glasses are Si-undersaturated and ne-normative. Normative albite (ab) and nepheline (ne) are higher in the Tarsia and LeS2 glasses (Fig. 9).

6. Discussion

6.1 Origin of the studied tephra layers and their relationships

The trachy-phonolitic glass compositions of the investigated tephra layers clearly exclude an origin from volcanism associated with the Aeolian Islands and nearby seamounts, Mount Etna and Pantelleria (Fig. 5a). Products with similar geochemical features have been erupted from different volcanic centers of the Roman Magmatic Province, including Vulsini, Vico and Roccamonfina (Peccerillo, 2005 and references therein). Trachytes and phonolites are also the typical products of Campanian volcanoes and were erupted at Ischia, Campi Flegrei and during the older periods of activity at Vesuvius (> 8 ka; Peccerillo, 2005; Santacroce et al., 2008). Assigning precise volcanic provenance to the

tephra units recorded at Palinuro and Tarsia is challenging firstly due to limited proximal exposure available for older volcanic eruptions following their destruction or burial by more recent caldera forming eruptions, for instance, the Campanian Ignimbrite and the Monte Epomeo Green Tuff at Campi Flegrei and Ischia respectively. Secondly, where proximal tephra units are recognized there is a lack of available glass geochemical data for reliable correlations at even a major element level.

Interestingly, the Valle del Crati tephra layer (Tarsia) and the lowermost investigated Palinuro tephra (LeS2) have very similar petrographic, geochemical and normative features, which suggests a common origin for these two levels. The uppermost Palinuro layer is clearly distinguished from the other two by its lower content in Na_2O and almost all incompatible elements and higher K_2O, CaO, MgO, Ba, Eu and Sr.

In the following section we focus on the integration of the Palinuro and Tarsia tephra levels into the Mediterranean tephrochronological framework by using our new geochemical data to assess their correlations with other tephra layers recorded in the region.

6.2 Comparison with X-5, X-6 and other correlated tephra layers

The tephra layers of the Cilento coastline (Palinuro) (LeS2 and LeS1) stratigraphically correlate with the CIL2 and CIL1 layers of Giaccio et al. (2012), which, in turn, have been correlated to X-6 and X-5 tephra markers, respectively. The correlation of LeS2 and LeS1 with CIL2 and CIL1 respectively is also confirmed by the major element composition of glasses (Fig.5b, Fig.10): LeS1 and CIL1 glass have homogeneous compositions characterized by relatively high K_2O, CaO and MgO contents, while LeS2 and CIL2 show a pronounced bimodality in the three elements. The consistent geochemical overlap between one population of the lower Palinuro tephra layer (LeS2) and the Tarsia tephra layer, coupled with their similar mineral phase compositions (Fig. 4 a and b) also enables us to correlate the Tarsia level of the Valle del Crati with CIL2 and thus the X-6 marker

tephra. The absence of the geochemical bi-modality in the Tarsia deposit, and specifically of the least evolved end-member of the CIL2/LeS2 tephra characterized by glasses with higher K_2O and MgO and lower contents of incompatible elements might relate to a change in the composition of erupted magma during the explosive event, with the least evolved component erupted towards the final stages of the eruption (e.g. as a consequence of an eruption from a zoned magma chamber). The absence of the high-Mg component in the Tarsia sequence might suggest that the upper portion of this volcaniclastic deposit has been partially eroded almost syn-eruptively. Below we integrate our new major and trace element glass data to explore new and existing tephra correlations associated with the X-5 and X-6 tephrostratigraphic markers.

6.2.1 LeS1 correlation

The K_2O/Na_2O vs CaO diagram(Fig. 5b) provides a useful first order discrimination between X-5 and X-6 glasses. TM-25 from LGdM (Wulf et al 2012), POP3 from Sulmona basin and CIL1 from Palinuro (Giaccio et al., 2012), all correlated to X-5 and have CaO > 2 wt% and K_2O/Na_2O > 2. The composition of LeS1 glasses clearly overlaps the compositional fields of these X-5 correlatives. Trace element data provides further confirmation that the LeS1 tephra layer can be attributed to the X-5/TM-25/POP3 eruptive event (Fig. 11a and b) and distinguished from slightly younger tephra units sharing similar major element chemistries.

At LGdM two levels (TM 24a, ca 101.8 ka BP and TM 24b, ca 102.8 ka BP), stratigraphically above the TM-25, were originally correlated to X-5 on the basis of major element chemistry (Wulf et al., 2007). However, subsequent studies (e.g., Wulf et al., 2012) demonstrated that TM-25 was a better stratigraphic, compositional and chronological match for the X-5 marine marker tephra, indeed new trace element glass data revealed that the TM-24 layers could be distinguished from the TM-25/X-5 layer on

the basis of their Ba and Sr contents at a given Th concentration. This re-appraisal has seen the refinement of the tephrostratigraphy in this time interval, having important implications for correlations associated within key tephrostratigraphic records. For instance at Lake Ohrid, tephra OT0702-8 remains correlated to TM-24a as proposed by Vogel et al. 2010) but can no longer be ascribed to the X-5 marine tephra as discussed by Leicher et al. (2015). Whilst in the Adriatic marine core PRAD1-2, tephra PRAD2525 previously correlated to TM-24a (Bourne et al., 2010) has been reassigned to a yet younger eruption from the Campanian volcanic zone TM-23-11 as recorded in LGdM (Giaccio et al., 2012; Bourne et al., 2015). In figure 12a and b we demonstrate that the glasses from the LeS1 tephra layer are indeed consistent with the fractionation trend observed in glasses of the X-5 correlatives, TM-25 and POP3, rather than the younger TM-24 layers, thus verifying the LeS1/X-5 correlation. New trace element data presented here for the LeS1 Palinuro tephra reinforce the identification of the X-5 in this region and crucially reinforces the chemical differences between the X-5/TM-25/POP3 and the younger TM-24 tephra layers. Consequently this helps strengthen the argument that the X-5/TM-25 can be distinguished from the younger TM-24 eruptive events as recorded at LGdM not only in terms of differing major element compositional variability. But the data presented here provides a further diagnostic geochemical tool for recognizing the X-5 layer and distinguishing it from slightly younger eruptions. Moreover, this demonstrates the importance of trace element data in tephrostratigraphic correlations and the caution that is necessary when correlating tephrostratigraphic records of different distal archives.

6.2.2 LeS2 and Tarsia correlation

On a K_2O/Na_2O vs CaO diagram (Fig. 5b) TM-27 (Wulf et al., 2012) and CIL2 tephra (Giaccio et al., 2012) layers, both correlatives of the marine marker X-6, have lower, though more variable, values of alkali ratio and calcium than correlatives of the X-5 tephra

discussed above. The Tarsia and LeS2 glass compositions analyzed here clearly reflect these geochemical features. The similarities in glass compositions evident in this diagram are also found in all the other major elements, and are particularly clear in MgO concentrations. The LeS2 and Tarsia tephra also have consistent major element glass compositions to those observed in the PRAD 2812 tephra layer recorded in the Adriatic marine core PRAD1-2, the I-9 layer of the Ionian Sea and the POP4 layer of the Sulmona basin (Fig. 5b and 10), all correlated to the X-6/TM-27 eruptive event (Insinga et al., 2014, Bourne et al., 2015, Regattieri et al., 2015).

At a trace element level the Tarsia and LeS2 glasses correspond well with the incompatible trace element concentrations seen in the glasses of the TM-27, I-9 and PRAD2812 layers (Bourne et al., 2015). Both the LeS2 and Tarsia tephra units have glasses showing significant enrichment in incompatible elements such as Zr, Nb and Th, whilst having strong depletions in Ba and Sr, all features which are consistent with the dominant end-member of the TM-27/PRAD2812/I-9 tephra (Fig. 11) (Insinga et al., 2014, Bourne et al., 2015).

Trace element concentrations, therefore, confirm the attribution of the LeS1 tephra to the X-5/TM-25 tephra marker and of LeS2 with X-6/TM-27 marker, as proposed by Marciano et al. (2008) and Giaccio et al. (2012) on the basis of major element geochemistry. Our geochemical investigations suggest that the thick volcaniclastic deposits recorded in the Valle del Crati is also a correlative the X-6 marker tephra. The most widely accepted age for this eruptive event would date this deposit in Tarsia as being108.9 ± 1.8 ka BP (Iorio et al., 2014). The seemingly erroneous luminescence age of this deposit of 42 ka produced by Carobene et al., (2006) might be responsible for the failed attempt to correlate this tephra to a well known eruptive event. Given the thickness of the deposit in northern Calabria, the Tarsia deposit is most certainly associated with an eruption responsible for widespread ash dispersal and was most likely to relate to one of the major Mediterranean

marker tephra horizons. From a geochemical stand point the levels of incompatible trace element enrichment in the Tarsia glasses far exceed anything observed in any of the younger Campanian derived, widespread, Late Pleistocene marker horizons including the Campanian Ignimbrite/Y-5 (Campi Flegrei), the MEGT/Y-7 (Ischia) and the Y-3 tephra (Campi Flegrei) (Fig. 13). These levels of enrichment are consistent with the most dominant population of evolved glasses observed in the correlatives of the X-6 tephra, TM-27 and PRAD2812.

Carobene et al. (2006) attributed the colluvium deposit in which the Tarsia pyroclastic level is embedded to the glacial MIS 4 conditions, while the underlying terrace is ascribed to the Last Interglacial (MIS 5.5). Dating the Tarsia tephra at ca.108 ka clearly means that we must refute that the colluvial deposit formed as a consequence of intense erosion associated with MIS 4 glacial conditions; but instead should be attributed to older stadial conditions associated with MIS 5.4 (Melisey 1 stadial), consistent with the X-6 tephra layers' position within high resolution palaeoclimate archives (Bourne et al., 2015; Regattieri et al., 2015).

7. Concluding remarks

The major and trace element micro-analyses of glasses from the Palinuro and Valle del Crati tephra layers provide new and important tephrostatigraphic data. Major element geochemical data here in the first instance re-affirms the correlation of the two volcaniclastic layers outcropping at Le Saline (Palinuro) to the X-5/TM-25 and X-6/TM-27 tephra markers (Giaccio et al., 2012), but crucially provide a more comprehensive trace element geochemical dataset which is essential for future more robust distal-distal tephra correlations throughout the Mediterranean region.

Geochemical investigation here point to a new occurrence of the X-6 marker tephra recorded as a volcaniclastic layer outcropping near the village of Tarsia (Valle del Crati,

Northern Calabria), thus providing new information on the areal distribution of this important tephra marker owing to it close association with the MIS 5.4 or Melisey 1 stadial conditions in the Mediterranean region (Wulf et al., 2012; Bourne et al., 2015; Regattieri et al., 2015). The correlation of Tarsia level with X-6 implies that its age (108.9 ± 1.8 ka) is much older than previously thought (< 42 ka, Carobene et al., 2006).

From the data presented in this work it is clear that X-5 and X-6 tephra markers are easily distinguishable on the basis of many trace elements, including the immobile HFSE. This makes the correlation with one or the other marker level possible even in scenarios where weathering might have modified the major elements concentration. This study demonstrates the benefits of detailed LA-ICP-MS microanalyses within tephrostratigraphic studies and provides new, important data for future studies on Quaternary stratigraphy in the central Mediterranean.

Acknowledgements

The authors would like to thank Prof. Salvatore Critelli (University of Calabria) for his assistance during the field work, Dr. Mariano Davoli (University of Calabria), Dr Victoria Smith (University of Oxford) and Dr Emma Tomlinson (Trinity College, Dublin) for their assistance with the SEM-EDS, EMP and LA-ICP-MS analyses, respectively, and Profs. Gaetano Robustelli and Fabio Scarciglia for constructive discussion. Finally, we are grateful to Giovanni Zanchetta and Biagio Giaccio for their comments and reviews, which greatly improved the quality of this manuscript. PGA was funded through a Reid Scholarship, Royal Holloway University of London with support from the Central Research Council, University of London and the NERC RESET consortium (project number NE/E015905/1). This paper forms the RHOXTOR contribution 045.

References

Albert, P.G., Tomlinson, E.L., Smith, V.C., Di Roberto, A., Todman, A., Rosi, M., Marani, M., Muller, W., Menzies, M.A. (2012). Marine-continental tephra correlations: Volcanic glass geochemistry from the Marsili Basin and the Aeolian Islands, Southern Tyrrhenian Sea, Italy. J. Volcanol. Geotherm. Res., 229-230, 74-94.

Albert, P.G., Hardiman, M., Keller, J., Tomlinson, E.L., Smith, V. C., Bourne, A.J., Wulf, S., Zanchetta, G., Sulpizio R., Müller U.C., Pross, J., Ottolini, L., Matthews, I.P., Blockley, S.P.E., Menzies, M.A. (2015). Revisiting the Y-3 tephrostratigraphic marker: a new diagnostic glass geochemistry, age estimate, and details on its climatostratigraphical context. Quat. Sci. Rev., 118, 105-121.

Allan, A.S.R., Baker, J.A., Carter, L., Wysoczanksi, R.J. (2008). Reconstructing the Quaternary evolution of the world's most active silicic volcanic system: insights from a similar to 1.65 Ma deep ocean tephra record sourced from Taupo Volcanic Zone, New Zealand. Quat. Sci. Rev., 27 (25–26), 2341–2360.

Amelio, M., Le Pera, E., Rizzo, V. (1997). Osservazioni stratigrafiche e mineralogiche sulle coperture detritiche della Valle di Maratea (Basilicata) Geogr. Fis. e Din. Quatern., 20, 13-23.

Blanc, A.C., Segre, A.G. (1953). Les formations quaternaires et les gisements paléolitiques de la côte de Salerno. Inqua, IV congr. Intern. (Roma- Pisa, 1953): Excursion dans les Abruzzes, Les Puilles et sur la côte de Salerno, 73-110.

Bourne, A., Lowe, J.J., Trincardi, F., Asioli, A., Blockley, S.P.E., Wulf, S., Matthews, I.P., Piva, A., Vigliotti, L. (2010). Distal tephra record for the last ca. 105,000 years from core PRAD 1-2 in the central Adriatic Sea: implications for marine tephrostratigraphy. Quat. Sci. Rev., 29, 3079-3094.

Bourne, A.J., Albert, P.G., Matthews, I.P., Wulf, S., Lowe, J.J., Asioli, A., Blockley, S.P.E., Trincardi, F. (2015). Tephrochronology of core PRAD1-2 from the Adriatic Sea: insights into Italian explosive volcanism for the period 200-80 . Quat. Sci. Rev., 116, 28-43.

Carobene, L., Dai Pra, G. (1991). Middle and Upper Pleistocene sea level highstand along the Tyrrhenian coast of Basilicata (Southern Italy).Il Quaternario, 4, 173-202.

Carobene, L., Cirrincione, R., De Rosa, R., Gueli, A.M., Marino, S., Troja, S.O. (2006) Thermal (TL) and optical stimulated luminescence (OSL) techniques for dating Quaternary colluvial volcaniclastic sediments: An example from the Crati Basin (Northern Calabria) Quatern. Int., 148, 149–164.

Critelli, S., Le Pera, E., Perrone, V., Sonnino, M. (1995) The sandstone memory of the Cenozoic evolution of the Southern Italy orogenic system. Geodinamica e tettonica attiva del sistema Tirreno-Appennino, Camerino, 96-98.

De Rosa, R., Dominici, R., Donato, P., Barca, D. (2008). Widespread syn-eruptive volcaniclastic deposits in the Pleistocenic basins of South-Western Calabria. J. Volcanol. Geotherm. Res., 177, 155-169.

Di Vito, M.A., Sulpizio, R., Zanchetta, G., D'Orazio, M. (2008). The late Pleistocene pyroclastic deposits of the Campanian Plain: new insights into the explosive activity of Neapolitan volcanoes. J. Volcanol. Geotherm. Res., 177, 19-49.

Donato, P., Albert, P., Crocitti, M., De Rosa, R. Menzies, M. (2013). Outcrops of X-5 and X-6 tephra markers along the Southern Tyrrhenian Coast of Italy. Goldschmidt 2013 Conference Abstracts, 1002.

Giaccio, B., Isaia, R., Sulpizio, R., Zanchetta, G. (2008a). Explosive volcanism in the central Mediterranean area during the late Quaternary-linking sources and distal archives. J. Volcanol. Geotherm. Res., 177, v-vii.

Giaccio, B., Isaia, R., Fedele, F.G., Di Canzio, E., Hoffecker, J., Ronchitelli, A., Sinitsyn, A., Anikovich, M., Lisitsyn, S.N. (2008b). The Campanian Ignimbrite and Codola tephra layers: two temporal/stratigraphic markers for the Early Upper Palaeolithic in southern Italy and eastern Europe. J. Volcanol. Geotherm. Res., 177, 208–226.

Giaccio, B., Messina, P., Sposato, A., Voltaggio, M., Zanchetta, G., Galdini, F., Gori, S., Santacroce, R. (2009). Tephra layers from Holocene lake sediments of Sulmona Basin, central Italy: implications for volcanic activity in Peninsular Italy and tephrostratigraphy in the central Mediterranean area. Quat. Sci. Rev., 28, 2710-2733.

Giaccio, B., Nomade, S., Wulf, S., Isaia, R., Sottili, G., Cavuoto, G., Galli, P., Messina, P., Sposato, A., Sulpizio, R., Zanchetta, G. (2012). The late MIS 5 Mediterranean tephra markers: a reappraisal from peninsular Italy terrestrial records. Quat. Sci. Rev., 56, 31-45.

Insinga, D.D., Tamburrino, S., Lirer, F., Vezzoli, L., Barra, M., De Lange, G.J., Tiepolo, M., Vallefuoco, M., Mazzola, S., Sprovieri, M. (2014). Tephrochronology of the astronomically-tuned KC01B deep-sea core, Ionian Sea: insights into the explosive activity of the Central Mediterranean area during the last 200 ka. Quat. Sci. Rev., 85, 63-84.

Iorio, M., Liddicoat, J., Budillon, F. Incoronato, A., Insinga, D.D., Cassata, W.S., Lubritto, C., Angelino, A., Coe, R.S., Tamburrino S. (2014). Combined palaeomagnetic secular variation and petrophysical records to time-constrain geological and hazardous events: an example from the eastern Tyrrhenian Sea over the last 120 ka. Glob. Planet. Change, 113 91–109.

Keller, J. Ryan, W.B.F., Ninkovich, D., Altherr, R. (1978). Explosive volcanic activity in the Mediterranean over the past 200,000 yrs as recorder in deep-sea sediments. Geological Society America Bulletin, 89, 591-604.

Leicher, N., Zanchetta, G., Sulpizio, R., Giaccio, B., Wagner, B., Nomade, S., Francke, A., Del Carlo, P. (2015). First tephrostratigraphic results of the DEEP site record from Lake Ohrid, Macedonia. Biogeosciences Discuss., 12, 15411-15460.

Lirer, L., Pescatore, T., Scandone, P. (1967) Livello di piroclastiti nei depositi continentali post-tirreniani del litorale Sud- tirrenico. Atti Soc. Gioenia Sc. Natur. Catania, 18, 85-115.

Lowe, J.J., Blockley, S., Trincardi, F., Asioli, A., Cattaneo, A., Matthews, I.P., Pollard, M., Wulf, S., 2007. Age modelling of late Quaternary marine sequences in the Adriatic: towards improved precision and accuracy using volcanic event stratigraphy. Continental Shelf Research, 27, 560-582.

Lucchi, F., Keller, J., Tranne, A.C. (2013) .Regional stratigraphic correlations across the Aeolian archipelago (southern Italy). In: Lucchi, F., Peccerillo, A., Keller, J., Tranne, C.A. & Rossi, P.L. (eds) 2013. The Aeolian Islands Volcanoes. Geological Society, London, Memoirs, 37, 55–81.

Marciano, R., Munno, R., Petrosino, P., Santangelo, N., Santo, A., Villa, I. (2008). Late quaternary tephra layers along the Cilento coastline (southern Italy). J. Volcanol. Geotherm. Res., 177, 227-243.

Mirigliano, G. (1949). Pliocene tra Licusati, S. Iconio e Porto degli Infreschi (Salerno). Boll. Soc. Natur. Napoli, 57, 60-71.

Mueller, W., Shelley, M., Miller, P., Broude, S. (2009). Initial performance metrics of a new custom-designed ArF excimer LA-ICPMS system coupled to a two-volume laser-ablation cell. J. Anal. At. Spectrom., 24, 209–214.

Paterne, M., Guichard, F., Labeyrie, J., Gillot, P.Y., Duplessy, J.C. (1986). Tyrrhenian Sea tephrochronology of the oxygen isotope record for the past 60,000 years. Marine Geology, 72, 259-285.

Paterne, M., Guichard, F., Labeyrie, J. (1988). Explosive activity of the south Italian volcanoes during the past 80,000 years as determined by marine tephrochronology. J. Volcanol. Geotherm. Res., 34, 153-172.

Paterne, M., Guichard, F., Duplessy J.C., Siani G., Sulpizio R., Labeyrie J. (2008). A 90,000-200,000 years marine tephra record of Italian volcanic activity in the central Mediterranean sea. J. Volcanol. Geotherm. Res., 177, 187-196.

Peccerillo, A. (2005). Plio-quaternary Volcanism in Italy. Springer-Verlag, Berlin, Heidelberg, 365 pp.

Regattieri, E., Giaccio, B.; Zanchetta, G., Drysdale, R.N. Galli, P., Nomade, S., Peronace, E., Wulf, S. (2015). Hydrological variability over the Apennines during the Early Last Glacial precession minimum, as revealed by a stable isotope record from Sulmona basin, Central Italy. J. Quat. Sci., 30, 19-31.

Santacroce, R., Cioni, R., Marianelli, P., Sbrana, A., Sulpizio, R., Zanchetta, G., Donahue, D.J., Joron, J.L. (2008). Age and whole rock–glass compositions of proximal pyroclastics from the major explosive eruptions of Somma-Vesuvius: A review as a tool for distal tephrostratigraphy. J. Volcanol. Geotherm. Res., 177,1-18.

Scandone, P., Lirer, L. (1966). Segnalazione di un livello piroclastitico nel Pleistocene superiore della costiera calabra e silentina. Boll. Soc. Natur. Napoli, 75, 201-204.

Scarciglia, F., Pulice, I., Robustelli, G., Vecchio, G. (2006). Soil chronosequences on Quaternary marine terraces along the northwestern coast of Calabria (Southern Italy). Quat. Int. 156–157, 133–155.

Siani, G., Sulpizio, R., Paterne, M., Sbrana, A. (2004). Tephrostratigraphy study for the last 18,000 14C years in a deep-sea sediment sequence for the south Adriatic. Quat. Sci. Rev., 23, 2485-2500.

Smith, V.C., Isaia, R., Pearce, N.J.G. (2011a). Tephrostratigraphy of post-15 kyr Campi Flegrei eruptions: implications for eruption history and chronostratigraphic markers. Quat. Sci. Rev., 30 (25–26), 3638–3660.

Smith, V.C., Pearce, N.J.G., Matthews, N.E., Westgate, J., Petraglia, M., Haslam, M., Lane, C., Korisettar, R., Pal, J. (2011b). Geochemical fingerprinting the widespread Toba tephra using biotite compositions. Quat. Int., 246, 97-104.

Sulpizio, R., Zanchetta, G., Paterne, M., Siani, G. (2003). A review of tephrostratigraphy in central and southern Italy during the last 65 ka. Il Quaternario, 16, 91-108.

Sulpizio, R., Zanchetta, G., D'Orazio, M., Vogel, H., Wagner, B. (2010). Tephrostratigraphy and tephrochronology of lakes Ohrid and Prespa, Balkans. Biogeosciences, 7, 3273-3288.

Sun, S.S. & McDonough, W.F. (1989). Chemical and isotopic systematic of oceanic basalts: implications for mantle composition and processes. in ''Magmatism in Ocean Basins'', A.D. Saunders &M.J. Norry, eds., Geol. Soc. Lond. Spec. Pub., 42, 313–345.

Tomlinson, E.L., Thordarson, T., Muller, W., Thirlwall, M., Menzies, M.A. (2010). Microanalysis of tephras by LA-ICP-MS- Strategies, advantages and limitations assessed using the Thorsmork ignimbrite (Southern Iceland). Chemical Geology, 279, (3-4), 73-89.

Tomlinson, E., Arienzo, I., Civetta, L., Wulf, S., Smith, V.C., Hardiman, M., Lane, C.S., Carandente, A., Orsi, G., Rosi, M., Muller, W., Thirwall, M.F., Menzies, M. (2012a). Geochemistry of the Phlegraean Fields (Italy) proximal sources for major Mediterranean tephras: implications for the dispersal of Plinian and co-ignimbritic components of explosive eruptions. Geochimica et Cosmochimica Acta, 93, 102-128.

Tomlinson, E.L., Kinvig, H.S., Smith, V.C., Blundy, J.D., Gottsmann, J., Muller, W., Menzies, M.A. (2012b). The Upper and Lower Nisyros Pumices: Revisions to the Mediterranean tephrostratigraphic record using micron-beam glass geochemistry. J. Volcanol. Geotherm. Res., 243-244, 69-80.

Vogel, H., Zanchetta, G., Sulpizio, R., Wagner, B., Nowaczyk, N. (2010). A tephrostratigraphic record for the last glacial-interglacial cycle from Lake Ohrid, Albania and Macedonia. J. Quaternary Sci., 25, 320-338.

Wulf, S., Kraml, M., Brauer, A., Keller, J., Negendank, J.F.W. (2004). Tephrochronology of the 100 ka lacustrine sediment record of Lago Grande di Monticchio (southern Italy). Quat. Int., 122, 7-30.

Wulf, S., Brauer, A., Mingram, J., Zolitschka, B., Negendank, J.F.W. (2007). Distal tephras in the sediments of Monticchio maar lakes. In: Principe, C. (Ed.), Geologia del Monte Vulture. Bollettino della Società Geologica Italiana, 105–122.

Wulf, S., Kraml, M., Keller, J. (2008). Towards a detailed distal tephrostratigraphy in the Central Mediterranean: the last 20,000 yrs record of Lago Grande di Monticchio. J. Volcanol. Geotherm. Res., 177, 118-132.

Wulf, S., Keller, J., Paterne, M., Mingrama, J., Lauterbach, S., Opitz, S., Sottili, G., Giaccio, B., Albert, P.G., Satowg, C., Tomlinson, E.L., Viccaro, M., Brauer, A. (2012). The 100-133 ka record of Italian explosive volcanism and revised tephrochronology of Lago Grande di Monticchio. Quat. Sci. Rev., 58, 104-123.

Zanchetta, G., Sulpizio, R., Giaccio, B., Siani, G., Paterne, M., Wulf, S., D'Orazio, M. (2008). The Y-3 tephra: a Last Glacial Stratigraphic marker for the central Mediterranean basin. J. Volcanol. Geotherm. Res., 177, 145-154.

Table titles

Table1: Occurrence of X-5- and X-6-related tephras in the Mediterranean area.

Table2: selected glass major (EMPA) and trace elements (LA-ICP-MS) for Le Saline and Tarsia tephra levels. Additional data available as supplementary material. 2× standard deviation is calculated on the reproducibility of MPI-DING StHs6/80 analyses.

Figure captions

Fig. 1- Distribution of X-5 and X-6- related tephra layers in the Central Mediterranean region. 1: Keller et al. (1978); 2: Paterne et al. (2008) and refs. therein; 3: Bourne et al. (2015); 4: Sulpizio et al. (2010); 5: Wulf et al. (2006); 6: Giaccio et al. (2012); 7: Lucchi et al. (2013); 8: Regattieri et al. (2015). Numbers in white squares indicate the thickness of tephra layers in centimetres; numbers in italics are referred to X-6- related tephras, bold numbers to X-5- related tephras. Red dots indicate the location of the tephra layers studied in this paper. The major Italian volcanic centres active during the late Quaternary are also shown.

Fig. 2- Schematic stratigraphic reconstructions of Le Saline and Tarsia successions (not to scale). Pictures of the outcrops and coordinates of the sampled outcrops are also shown.

Fig. 3- SEM- BSE (Back Scattered Electrons) pictures of studied tephra deposits. a) vesiculated pumice with a sanidine crystal in LeS1 level; b) glass shard in LeS2; c) glass shards and small pumices in the Tarsia deposit; d) coarse (>1 mm) pumice in the Tarsia deposit.

Fig. 4- Plagioclase (a) and pyroxene (b) composition of Le Saline and Tarsia tephra deposits.

Fig 5 a) Total alkalies vs Silica (TAS) diagram for the glasses of Palinuro and Tarsia tephra deposits. Compositional fields of Italian volcanoes are also outlined for comparison by data from Peccerillo (2005) and references therein. B) alkali ratio vs CaO. Compositional fields of tephra deposits related to X-5 and X-6 are also outlined for comparison. *: Wulf et al. (2012); **: Giaccio et al. (2012); ***: Regattieri et al. (2015); °: Insinga et al. (2014). Compositional data for X-5 and X-6 are from Keller et al. (1978). Error bars indicate 2× standard deviation based on reproducibility of MPI-DING StHs6/80 analyses.

Fig. 6- Major elements vs Silica Harker diagrams for the glasses of Palinuro and Tarsia. Error bars indicate 2× standard deviation based on reproducibility of MPI-DING StHs6/80 analyses.

Fig. 7- Trace elements vs Silica Harker diagrams for the glasses of Palinuro and Tarsia. Error bars for trace elements are smaller than the symbols (see table 2 for values); error bar for Silica indicates 2× standard deviation based on reproducibility of MPI-DING StHs6/80 analyses.

Fig. 8- Incompatible elements (a) and Rare Earth Elements (b) spider diagrams for the glasses of Palinuro and Tarsia (normalization after Sun and McDonough, 1989). Insert in (b) is the Eu anomaly.

Fig. 9-Norrmative nefeline (ne) and albite (ab) for the glasses of Palinuro and Tarsia.

Fig. 10- Comparison between the Palinuro and Tarsia volcaniclastic levels studied in this paper and X-5 and X-6 related tephra layers. *: Giaccio et al. (2012); **: Wulf et al.(2012); ***: Bourne et al. (2015); °: Regattieri et al. (2015); °°: Insinga et al. (2014). Error bars indicate 2× standard deviation based on reproducibility of MPI-DING StHs6/80 analyses.

Fig. 11- Trace elements concentration for Le Saline and Tarsia levels glass. Compositional fields of other X-5- and X-6- related tephras are also drawn for comparison. *: Wulf et al. (2012); **: Giaccio et al. (2012); ***: Bourne et al. (2015); °: Insinga et al. (2014). Error bars for trace elements are smaller than the symbols (see table 2 for values).

Fig. 12- Trace elements composition of LeS1 glass compared to other X-5-related tephras. Data for TM24 tephra are also reported for comparison. See text for discussion. *: Wulf et al. (2012); ** Giaccio et al. (2012). Error bars for trace elements are smaller than the symbols (see table 2 for values).

Fig. 13- Comparison between the trace elements contents of LeS2-Tarsia level with those of Y-3 (Campi Flegrei, data from Albert et al., 2015), Y-5 (Campanian Ignimbrite, Campi Flegrei, data from Tomlinson et al., 2014) and Y-7 (Mount Epomeo Green Tuff, Ischia, data from Tomlinson et al., 2012a).

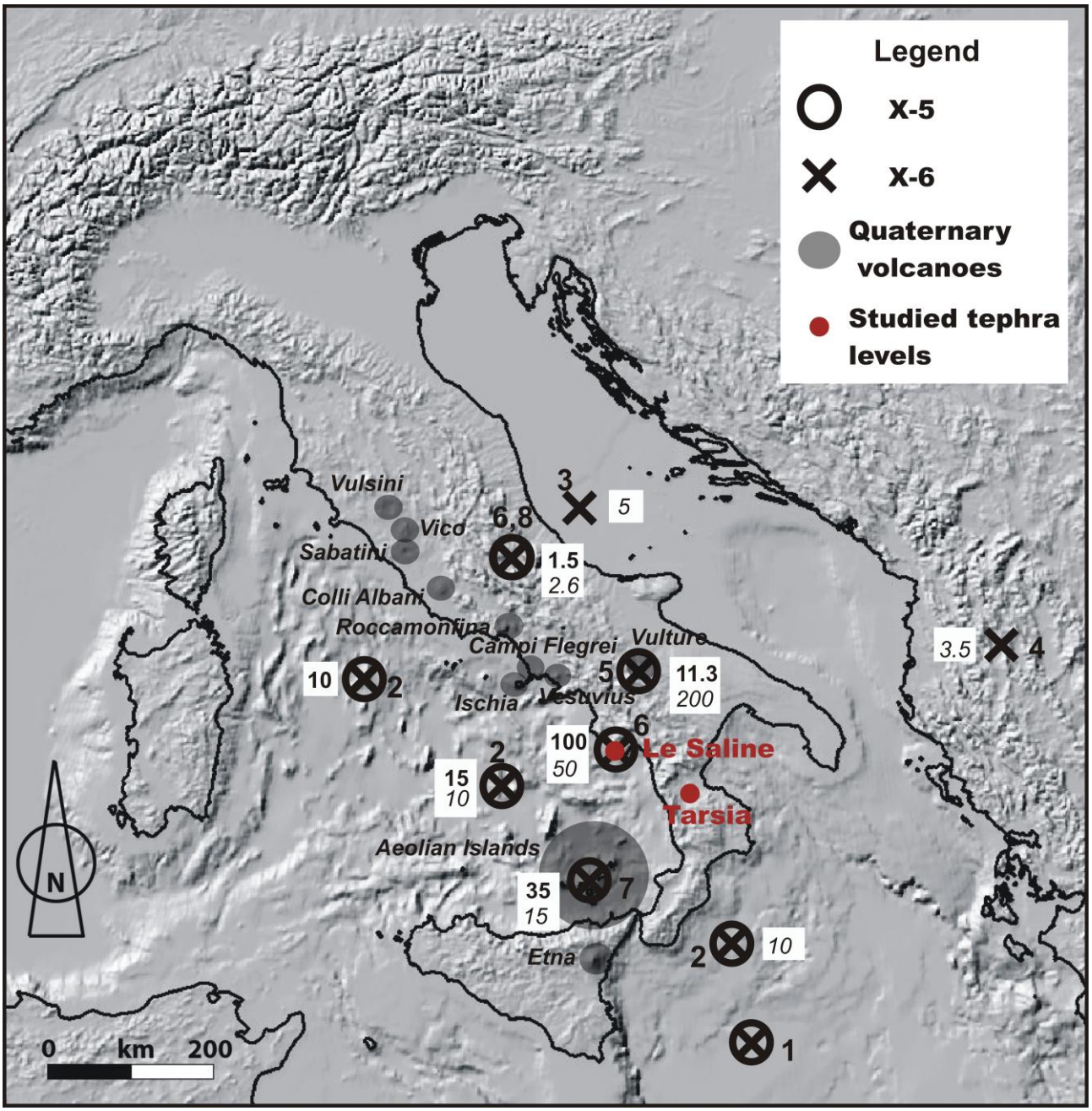
Legend
X-5
X-6
Quaternary volcanoes
Studied tephra levels
Vulsini
Vico
Sabatini
Colli Albani
Roccamonfina
Campi Flegrei
Vulture
Ischia
Vesuvius
Le Saline
Tarsia
Aeolian Islands
Etna
3
5
6,8
1.5
2.6
10
2
5
11.3
200
3.5
4
6
100
50
2
15
10
35
15
7
2
10
1
N
0
km
200

Figure 1

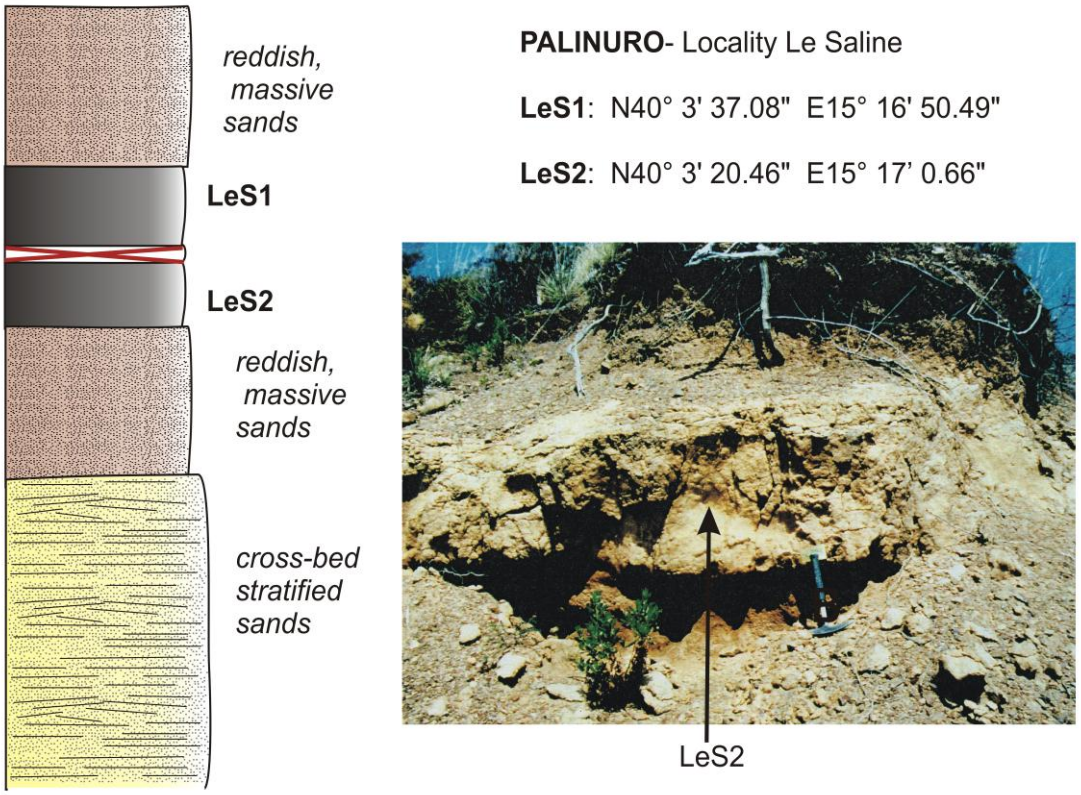

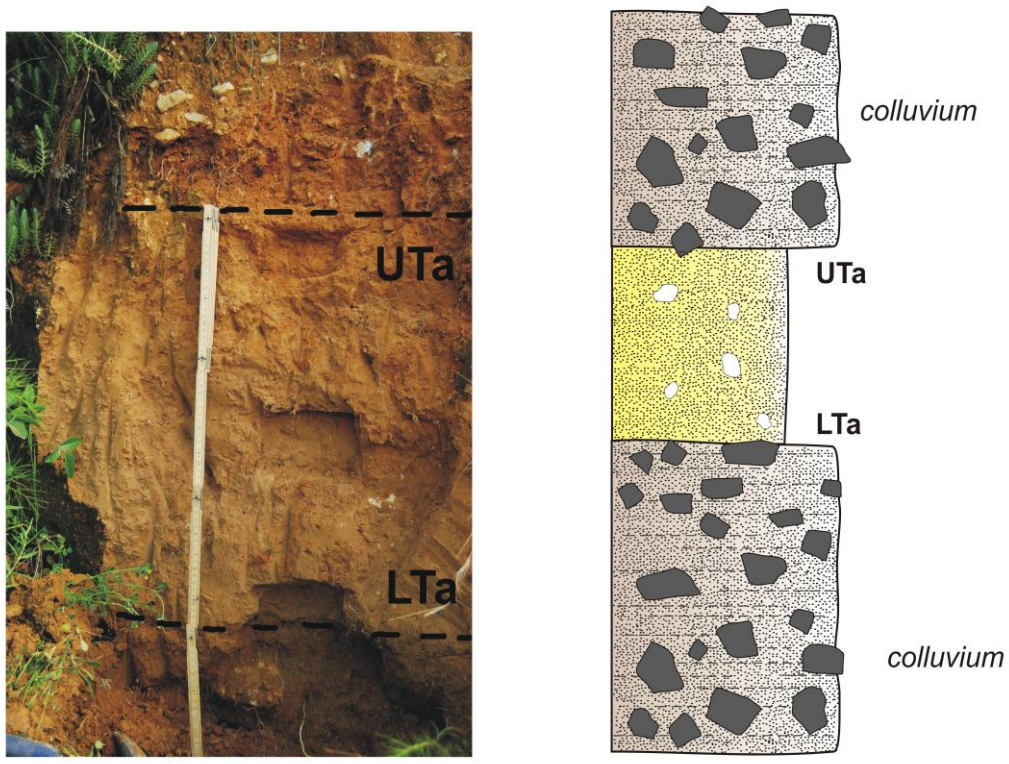

Figure 2

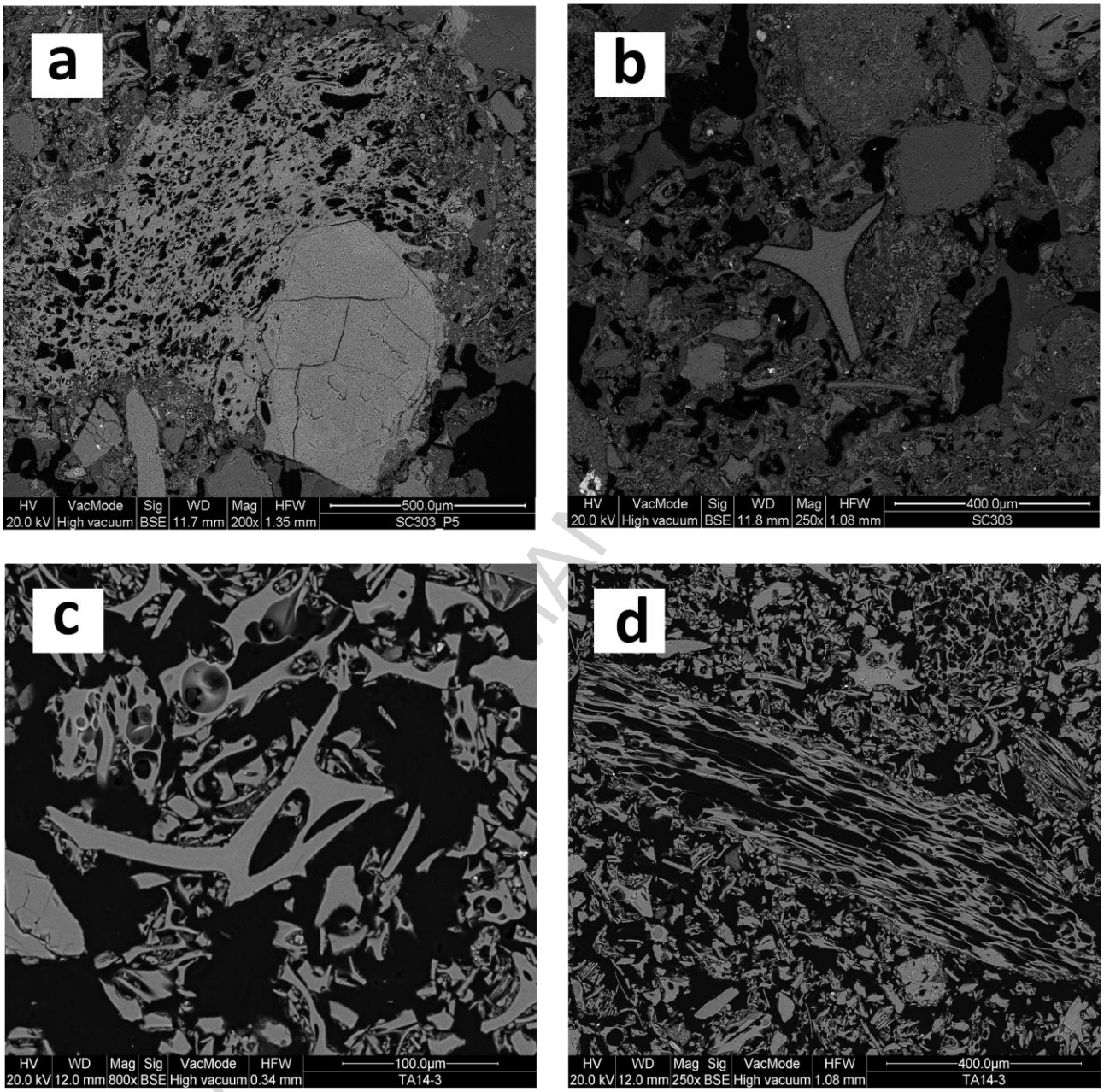

Figure 3

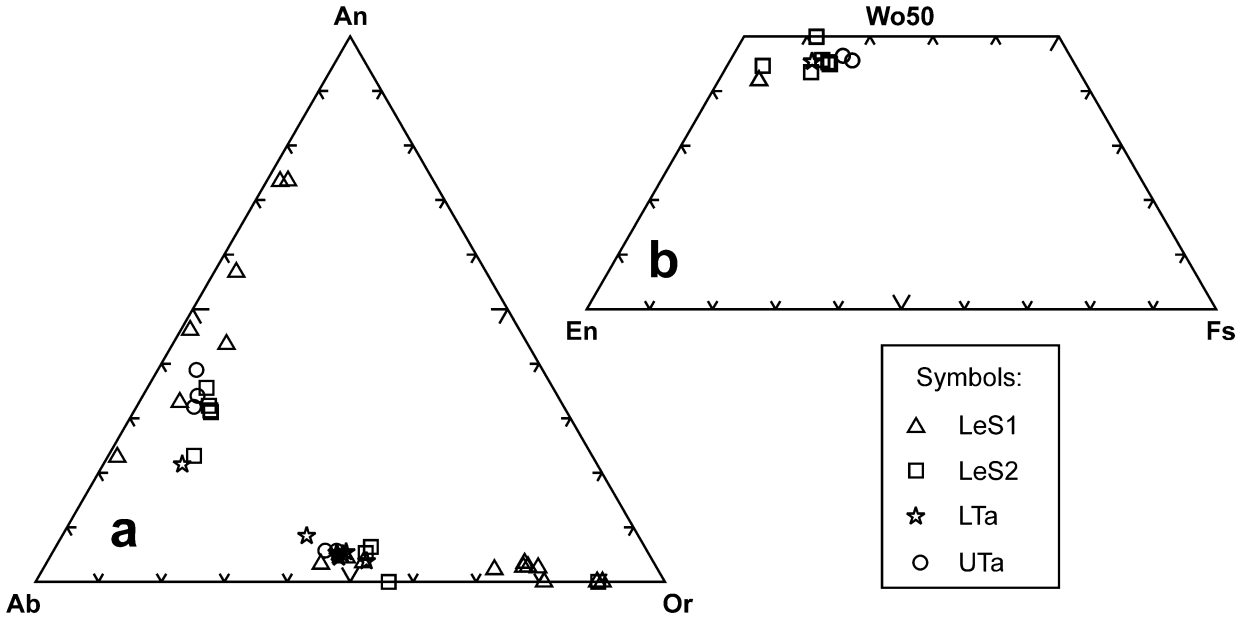

Figure 4

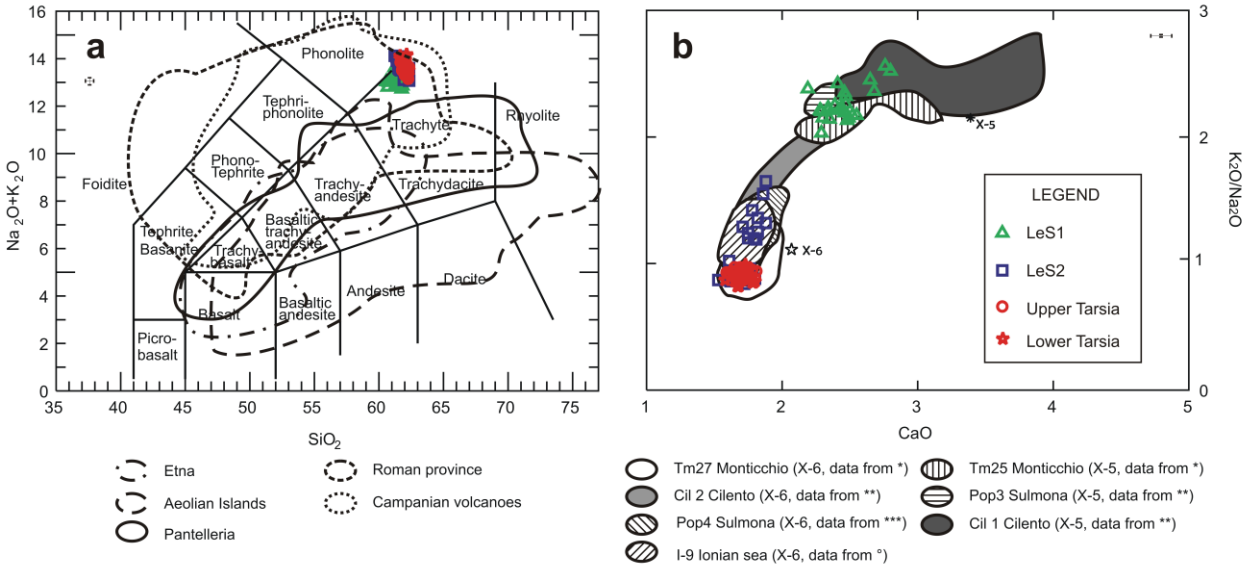

Figure 5

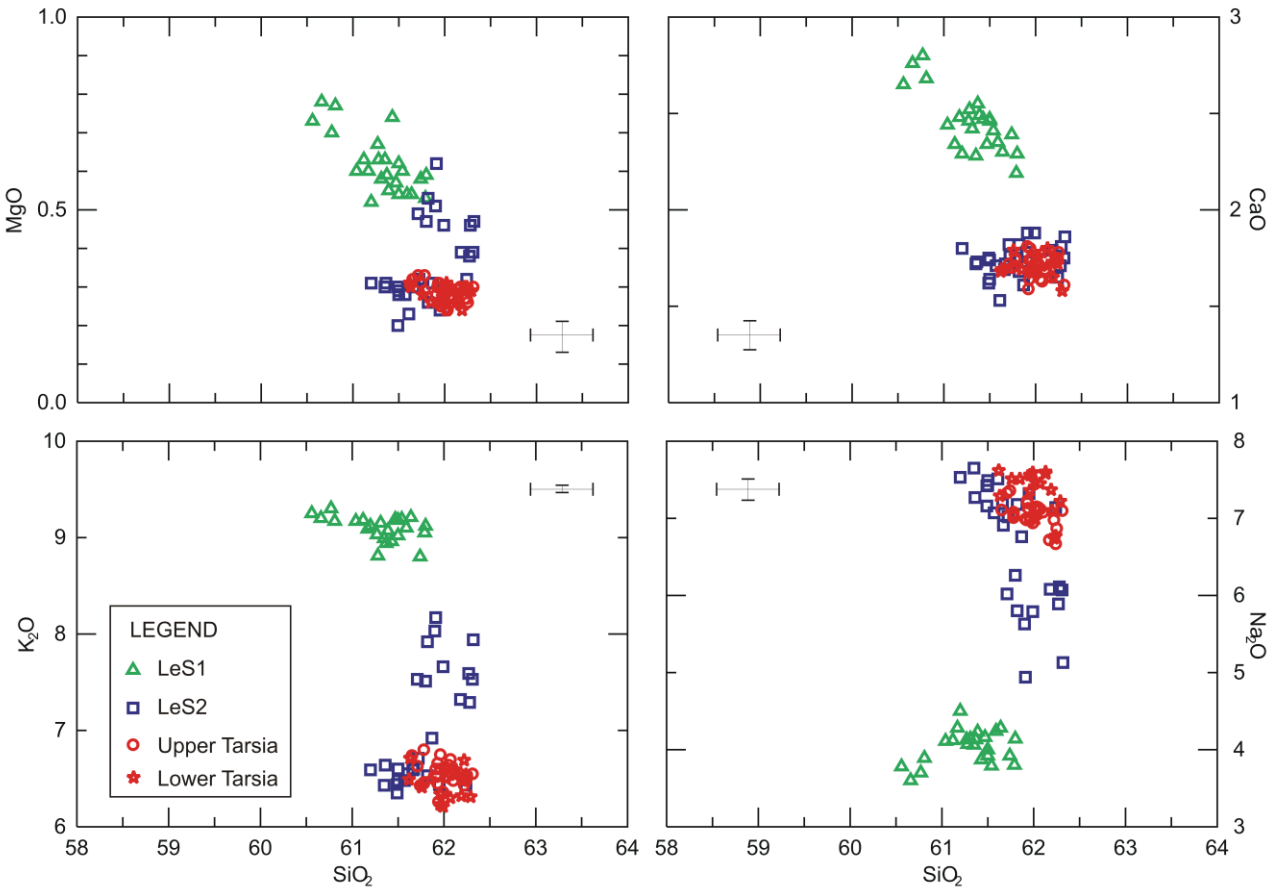

Figure 6

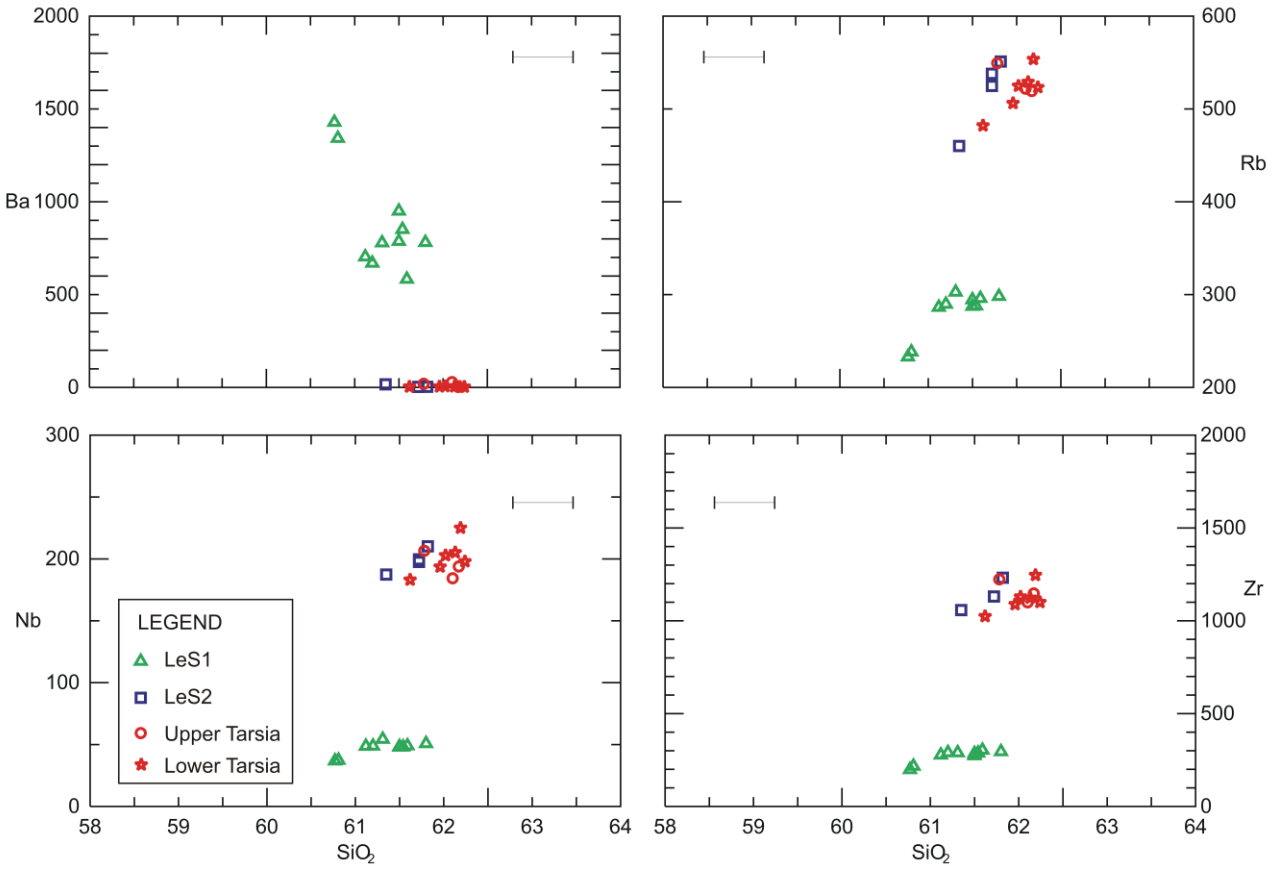

Figure 7

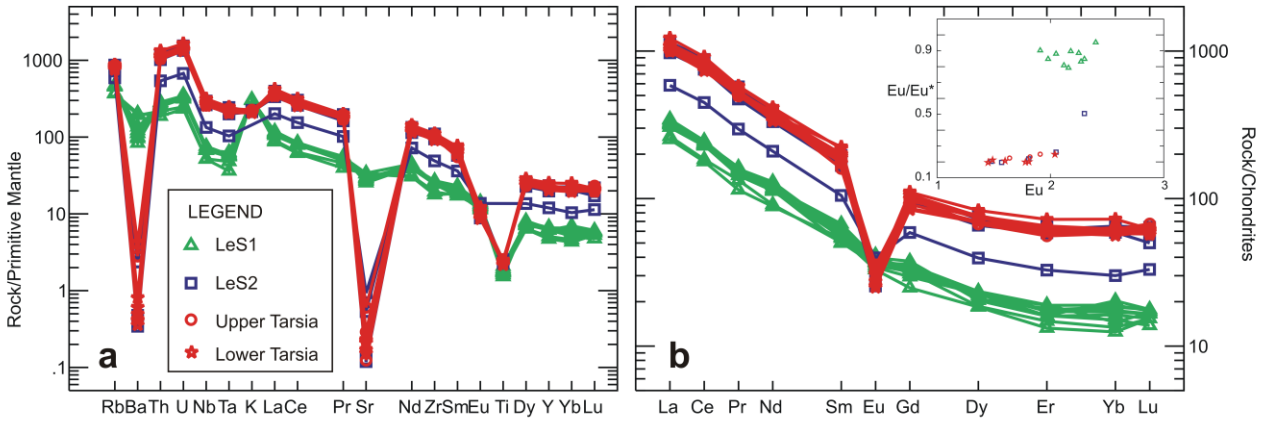

Figure 8

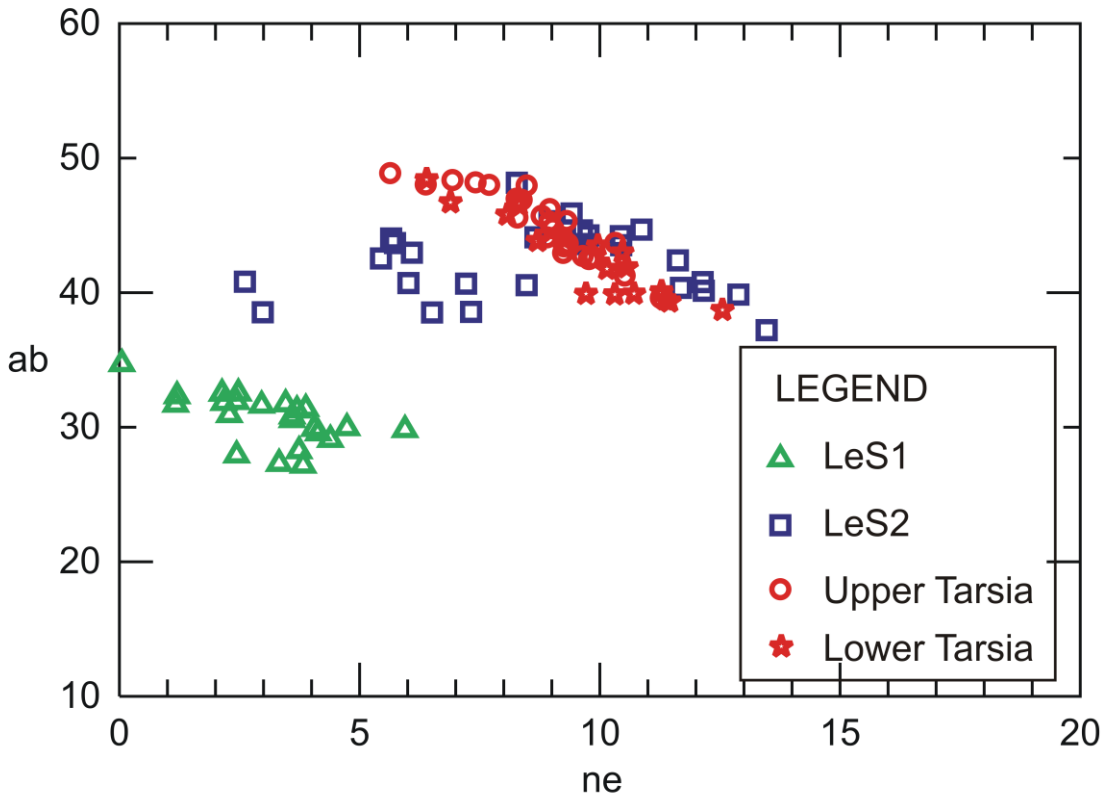

Figure 9

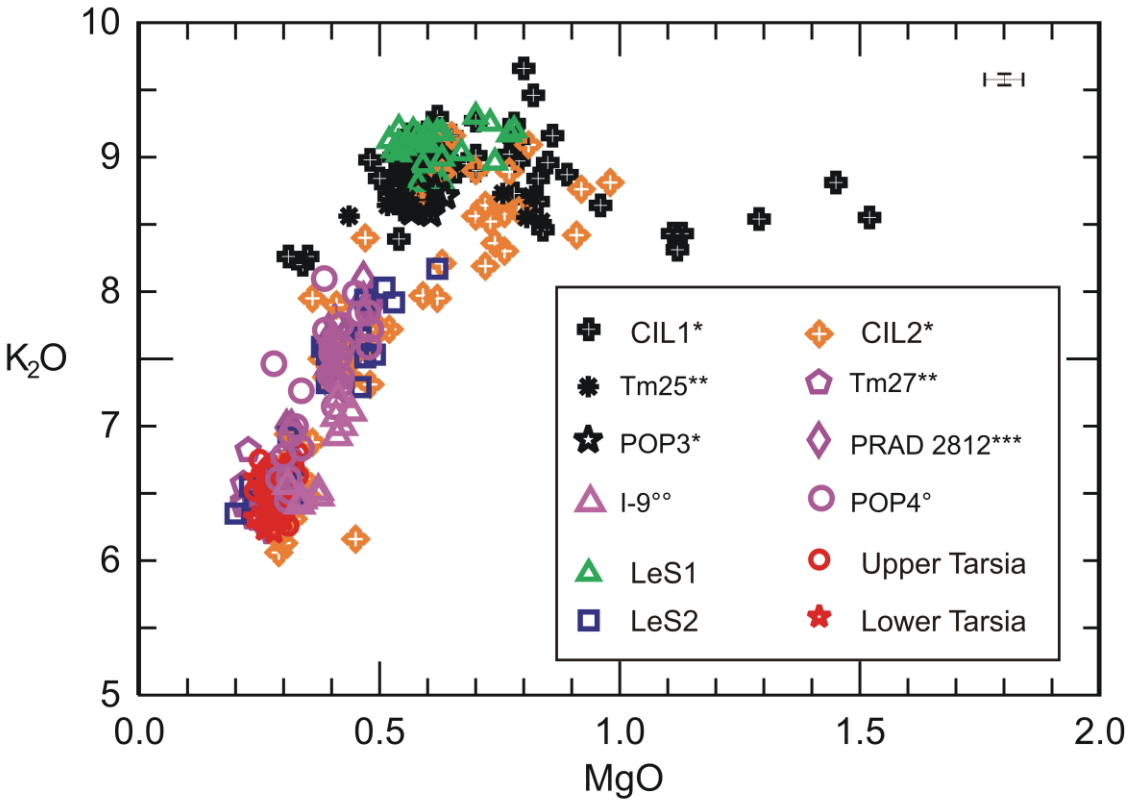

Figure 10

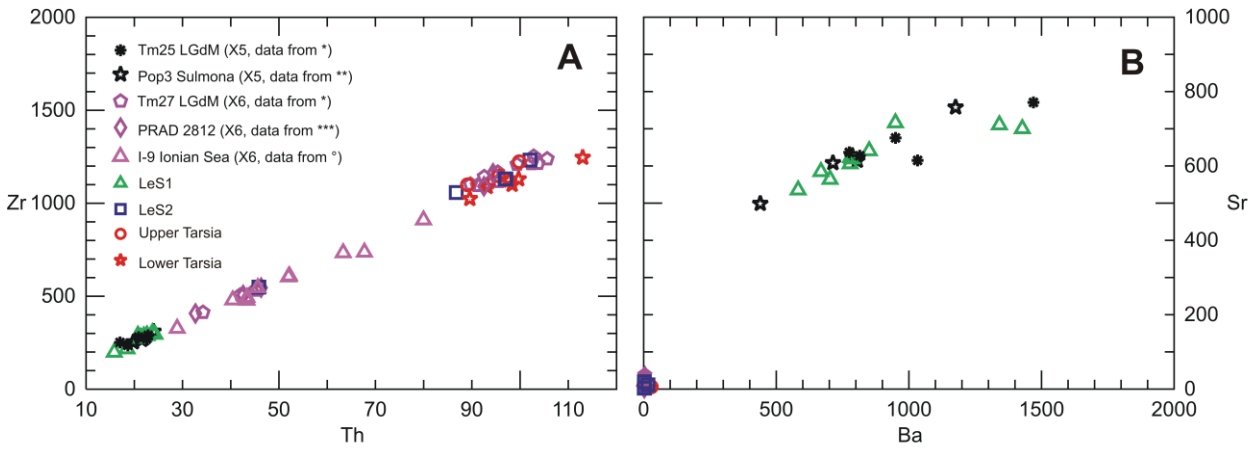

Figure 11

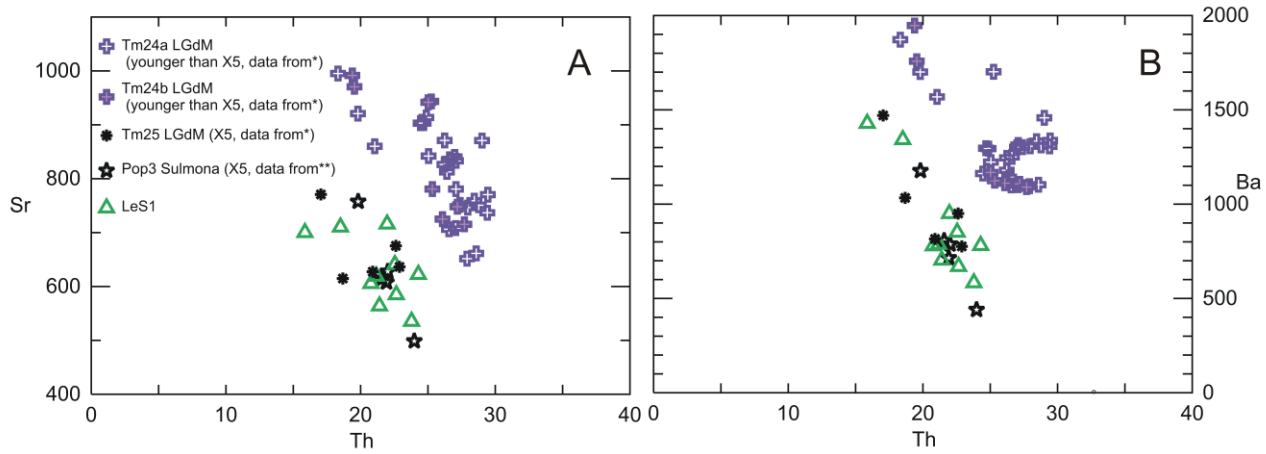

Figure 12

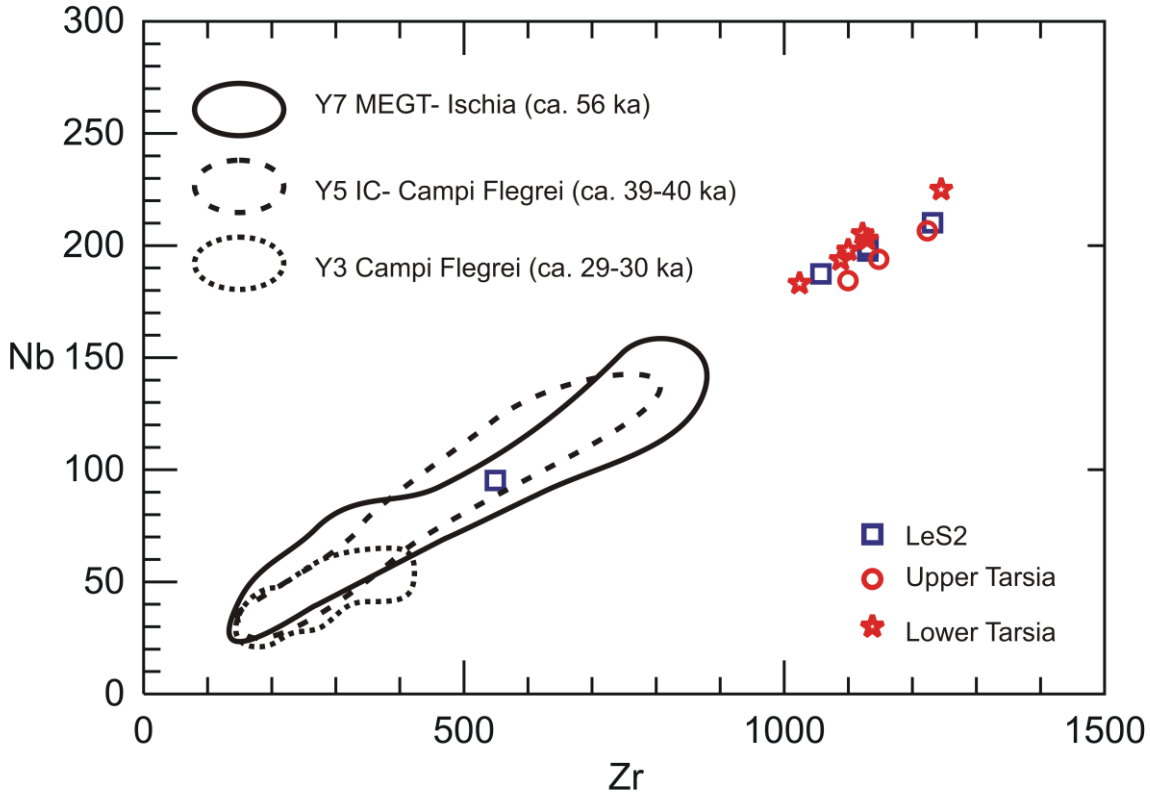

Figure 13

Table 1

Tephra	Record	Method	Age (ka)	Reference
X-5				
TM-25	Lago Grande di Monticchio	Varve Chronology	105.5 ± 5.3	Wulf et al., 2012
POP-3	Sulmona Basin	$^{40}Ar/^{39}Ar$	106.2 ± 1.3	Giaccio et al., 2012
C-27	Tyrrhenian and Ionian Seas: KET 80-04, DED 87-08, KET 82-22	Orbitally Tuned Oxygen isotope record	103.5	Paterne et al., 2008
X-6				
POP-4	Sulmona Basin	Stal-Age algorithm	109± 1.5	Regattieri et al., 2015
TM-27	Lago Grande di Monticchio	Varve Chronology	108.3 ± 5.4	Wulf et al., 2012
T-1	Tyrrhenian Sea C1202	40Ar/39Ar	108.9 ± 1.8	Iorio et al., 2014
C-31	Tyrrhenian and Ionian Seas: KET 80-04, DED 87-08, KET 82-22	Orbitally Tuned Oxygen isotope record	107	Paterne et al., 2008

Table 2

	LeS1		LeS2		LTa		UTa		
	15B_1	36D_1	26D_2	13B_1	2A_1	27C_1	1A_1	7A_1	***2 STDV***
SiO_2	61.54	61.50	61.82	61.72	62.19	61.62	62.17	62.10	***0.64***
TiO_2	0.45	0.35	0.49	0.50	0.52	0.49	0.51	0.52	***0.08***
Al_2O_3	18.71	18.88	18.51	18.57	18.09	18.34	18.71	18.49	***0.4***
FeO	3.15	3.07	3.16	3.07	3.33	3.02	2.99	3.08	***0.23***
MnO	0.16	0.17	0.38	0.33	0.28	0.43	0.40	0.28	***0.07***
MgO	0.60	0.54	0.26	0.32	0.24	0.31	0.30	0.27	***0.08***
CaO	2.41	2.47	1.68	1.76	1.65	1.68	1.65	1.69	***0.15***
Na_2O	3.79	4.00	7.18	7.02	7.37	7.62	6.72	7.08	***0.28***
K_2O	9.19	9.02	6.53	6.71	6.32	6.49	6.55	6.48	***0.07***
Total Alkalis	12.98	13.02	13.71	13.73	13.69	14.10	13.28	13.56	***0.3***
K_2O/Na_2O	2.42	2.26	0.91	0.96	0.86	0.85	0.97	0.91	***0.02***
Rb	288	287	551	538	554	482	519	522	***0.85***
Sr	640	716	3	3	3	5	3	6	***7.98***
Y	30	30	106	106	115	92	102	98	***0.59***
Zr	287	284	1232	1131	1245	1024	1147	1099	***4.18***
Nb	48	48	210	200	225	183	194	184	***0.21***
Ba	851	949	3	2	3	3	3	29	***11.22***
La	75	82	272	265	290	236	264	239	***0.33***
Ce	142	151	537	516	559	450	506	471	***0.94***
Pr	15	15	54	51	55	47	50	47	***0.31***
Nd	53	61	174	181	193	160	179	171	***0.70***
Sm	10	9	29	29	33	27	28	24	***0.76***
Eu	2	2	2	2	2	1	2	2	***0.12***
Gd	6	7	21	20	23	17	20	20	***0.54***
Dy	6	6	19	19	21	18	19	17	***0.23***
Er	3	3	11	10	12	10	10	9	***0.12***
Yb	3	3	11	11	12	10	11	10	***0.27***
Lu	0	0	2	1	2	2	2	1	***0.07***
Ta	2	3	10	9	10	8	9	9	***0.07***
Th	23	22	102	97	113	90	96	89	***0.17***
U	7	7	32	30	35	28	29	29	***0.09***

Highlights

- Glass major and trace elements are presented for 3 tephras (Palinuro and Tarsia)
- Tephra LeS1 (Palinuro) unequivocally correlates to X-5
- Tephra LeS2 (Palinuro) and Ta (Tarsia) correlate to X-6
- Our findings are crucial for tephrostratigraphic studies in the Mediterranean area